Indian Journal of Basic and Applied Medical Research; June 2021: Vol.-10, Issue- 3, P. 262 - 271
DOI: 10.36848/IJBAMR/2020/29215.55796

Review Article

Finite Element Method in Orthodontics

Dr. Purnima Bhave, Dr. Falguni Mehta, Dr. Renuka Patel, Dr. Harshik Parekh, Dr. Rahul Trivedi

Name of the Institute/college: Government Dental College and Hospital, Ahmedabad
Corresponding author: Dr. Purnima Bhave; Email id: purnimabhave9216@gmail.com

Abstract:
The finite element method (FEM) involves a series of mathematical process that calculates the stress distribution in each element. It allows the calculation of stress resulting from external force, pressure, thermal change as well as other forces. This method is extremely useful for simulation of mechanical process of objects as well as human body that that is complicated to be measured in vivo. The data thus obtained can be visualized with the help of software to study a various boundary condition. This paper emphasizes on application of this method in the field of orthodontics.
Keywords: finite element method , mathematical process

Introduction:
The finite element method (FEM) is basically a numerical method which scrutinize stresses and deformations of the structures having various geometries. It was originally introduced as a method for decoding mechanical problems, which was later utilized as a general procedure for all physical problems [1]. It reveals the superimposed structures, and provides the material properties of an object. It also enables location determination, magnitude and direction of an applied force, that can't be measured physically.
Forces with various range of magnitudes and directions can be virtually applied. In dentistry, finite element analysis has been used to analyse a broad variety of subjects such as the structure of teeth, implants, biomaterials, and root canals.

Basic steps in finite element method[2]

(1) Pre-processing:

Construction of the Geometric model

Construction of the Geometric model: Aim of this phase is to represent geometry in terms of points, lines, areas and volume.

This can be achieved by:

3D – CT scanner: Used for modelling complex structures or living tissues.

3D – Laser scanner: For modelling inanimate objects.

(2) Conversion of Geometric model to Finite Element model

Discretization is the process of dividing problem into several small elements, connected with nodes. All basic elements must be numbered to maintain connectivity.

The elements could be in different shapes and dimensions. It must be taken care of that there should be no overlapping elements. Elements should be connected only at the key points, which are termed **nodes**. The joining of elements at the nodes and removal of duplicate nodes is termed as **'Meshing'**.

(3) Assembly / Material Property data representation:

Equations are developed for each element present in mesh and assembled into a set of equations that model the properties of the entire system. Minimum material properties required are Poisson's ratio and Young's modulus.

	Young's modulus (Nm^{-2})	**Poisson's ratio**
Tooth	$19.6 * 10^9$	0.3
Pdl	$5*10^6$	0.45
Cancellous bone	$0.5*10^9$	0.3
Cortical bone	$13.7*10^9$	0.3

(4) Defining the Boundary Conditions:

Boundary conditions means that suppose an element is constructed on the computer and a force is applied to it, it will act like a free-floating rigid body and will undergo a translatory or rotatory motion or a combination of the two without experiencing deformation.

To study its deformation, some degrees of freedom must be restricted (movement of the node in each direction x, y, and z) for some of the nodes. Such constraints are termed boundary conditions.

(5) Loading configuration:

Application of force at various points of geometry and its configuration.

(6) Processing:

Solve the system of linear algebraic equation. The stresses are determined from the strains by Hooke's law. Strains are derived from the displacement functions within the element Combined with Hooke's law.

(7) Post-Processing:

The output usually consists of nodal values of the field variables. Itis primarily in the form of color-coded maps. The analysis is confirmed by interpreting these maps.

USES IN ORTHODONTICS

(I) ORTHOPAEDIC FORCES

30 mandibular landmarks were digitized to evaluate morphological changes of Mandible in pre-pubertal and pubertal patients with Class II Division 1 malocclusions treated with Twin-block appliances[3]. For shape change, all configurations were highly isotropic over the entire mandibular nodal mesh. Twin block appliance therapy may involve developmental modulations at the condylar cartilage, remodelling of the ramus and corpus, and osteogenic deposition in dentoalveolar regions. Localization of growth in the condylar neck with concomitant remodelling of the coronoid process may reflect the correction of mandibular form achieved with Twin block.

Effects of a fixed functional appliance (Forsus Fatigue Resistant Device) on the mandible were studied with 3-D finite element analysis[4]. Both the von Mises and principal stresses increased many more times in the teeth than in the mandible at the resting stage. Increase in the von Mises stress were by 3 times in the cortical bone and by more than 2 times in the condyle. Maximum principal stress increased by more than 2 times in the cortical bone and by more than 3 times in the condyle.

Effects of the Class II activator and the Class II activator high-pull headgear (HG) combination on the mandible were evaluated with 3D finite element stress analysis[5]. The mandibular body was subjected to higher stresses than the condylar region. The maximum stress values were obtained in the muscle attachment regions. The medial side and the top of the coronoid process were the most stressed regions.

Stress and deformation distribution patterns on the maxillary bone structure were studied using the finite element method by simulation of different vertical and anteroposterior positions of the expansion screw on the hyrax expander appliance[6]. 6 distinct finite element method models were created to simulate different positions of the expansion screw. The stress was concentrated in the anterior region, close to the incisive foramen, scattering through the palate posterolaterally. When the screw is closer to the occlusal plane and in a more anterior position, more stress was located around the incisive foramen. More posterior positions resulted in stress generation around the pterygoid pillars. At all simulations, the midpalatal suture showed a V-shaped expansion, with the vertex superior in the coronal view and posterior in the axial view.

(2) CENTER OF RESISTANCE

Change in position of CR associated with alveolar bone loss was studied when 1N (5.5 mm apical to the incisal edge which is location of bracket) force is applied[7]. 6 models of an upper central incisor with 1-8 mm of alveolar bone loss were created. CR located approximately 5 mm apical to alveolar crest in no bone loss model, but the position of CR decreased to 1.46 mm for 8 mm of alveolar bone loss. As CR moves apically with the alveolar bone loss, the distance between CR and the alveolar crest decreases.

Position of CR for 4 and 6 maxillary anterior teeth respectively and the full maxillary dentition (200 g force) was studied[8]. Location of CR for 4 teeth group, 6 teeth group, and the full dentition group were found out to be at 13.5 mm apical and 12.0 mm posterior, 13.5 mm apical and 14.0 mm posterior, and 11.0 mm apical and 26.5 mm posterior to the incisal edge of the upper central incisors respectively.

A study of 3-D model of maxillary 4 incisors to evaluate CR during simultaneous intrusion (15g) and retraction (120g) concludes following[9]. CR was located in the mid-sagittal plane at 6 mm apical and 4 mm posterior to a line perpendicular to the occlusal plane from the labial alveolar crest of the central incisor.

Model of 14 mandibular teeth were examined to determine the location of CR. CR was located for 4 and 6 mandibular anterior teeth, and complete mandibular dentition. 200 g retraction and intrusion forces were applied 0 mm, 5 mm, 10 mm, 15 mm and 20 mm in vertical direction from mandibular central incisors to the lingual and apical directions respectively[10]. The position of the CR for the 4 mandibular anterior teeth in vertical and anteroposterior direction was 13.0 mm apical and 6.0 mm posterior to the incisal edge of the mandibular central incisors respectively. The location of the CR for the 6 mandibular anterior teeth in vertical and anteroposterior

direction was 13.5 mm apical and 8.5 mm posterior to the incisal edge of the mandibular central incisors respectively. For the whole mandibular dentition CR was located 13.5 mm apically and 25.0 mm posterior to the incisal edge of the mandibular central incisors for vertical and anteroposterior directions respectively.

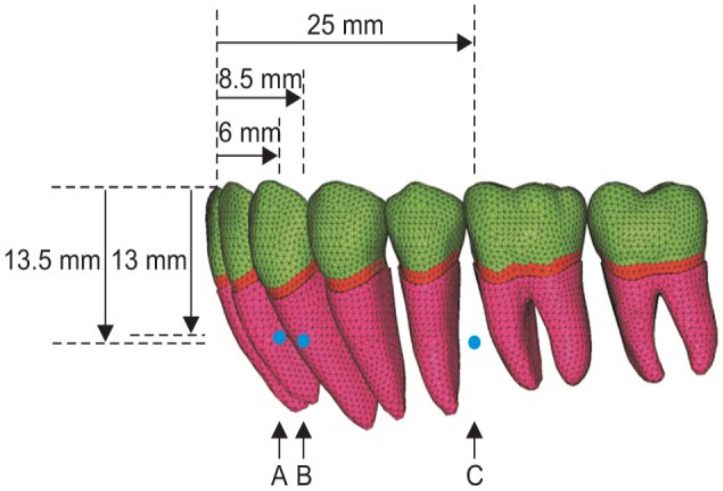

Figure 1: Various center of resistance for mandibular dentition

(3) LOOP BIOMECHANICS

The study on effect of different loop positions on the mechanical properties of the Opus loop and other L-shaped loops with a 12-mm inter-bracket distance and 10 mm of loop height and width reveals following results[11]. No change in moment was observed when T-loop was placed <1/3rd of the distance. M/F ratio obtained by upright L loops were greater than the angulated L loops (L90>L70; LC90>LC70; Opus90>Opus70). The Opus90 could obtain M/F ratio higher than the Opus70. The highest M/F ratio for a coiled L-loop was found when located at centre of inter-bracket distance. Upright L-loops achieved maximum M/F ratios when loops were positioned around the centre, whereas for backward tipped L and T-loops acquired maximum ratios when they were placed close to the canine brackets.

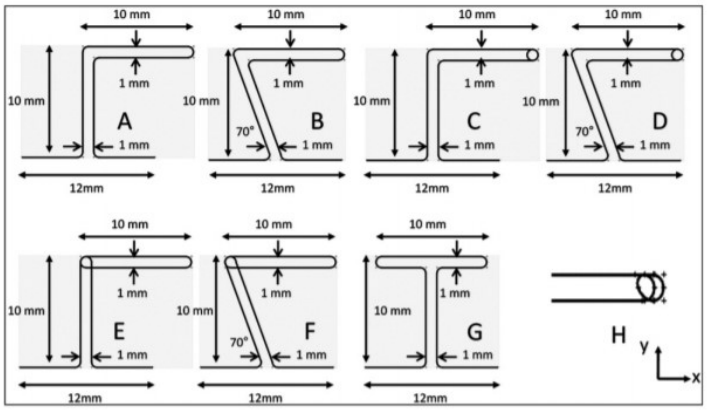

Figure 2: Comparisions of Opus loop and other L-shaped loops

Forces, moments and M/F ratios of the opus, L, T and vertical helical closing loop (VHC loop) were compared and examined with FE method[12]. Loops were made up of 0.016 x 0.022-inch rectangular stainless-steel wire. The highest horizontal and vertical forces were produced by the L–loop (with and without preactivation bends) and the lowest forces were produced by the VHC loop. Loops with preactivation bends generate distinct changes in the M/F ratio whereas loops without bends produce low but constant, M/F ratios. Of the loops without preactivation bends the opus and T-loop had the highest M/F ratios (7.20 – 7.67 mm at the anterior ends).

Biomechanical properties of snail loop and compared it with teardrop and opus loops were evaluated. 13 finite element models were constructed[13]. Opus loop produced highest inherent M/F ratio and least load deflection rate. Addition of 20°gable bends in snail loop made of 0.017 × 0.025" S.S or 0.019 × 0.025" TMA wire generate M/F ratio required to obtain bodily movement with acceptable F/D rate.

The effects of variable vertical loop height and design on its force characteristics at various amounts of activation were examined[14]. Double vertical open loop (DVOL) and double vertical helical open loop (DVHOL) with each one in two heights (6 mm, 7 mm respectively) were 3-D modelled. The minimum force was produced by DVHOL (7mm) at 0.1 mm activation (1.06E-01 N). The maximum force (2.2199 N) was delivered by DVOL (6mm) at 1 mm activation. For each activation force levels are in following order: DVOL 6 mm > DVOL 7 mm > DVHOL 6 mm > DVHOL 7 mm. Addition of a helix in DVOL and increasing the height can reduce force levels.

Comparative study of biomechanical features of closed helical loop (2 × 7 mm) and T-loop (6 × 2 × 7 mm) during retraction in lingual orthodontics concludes that the T-loop has increased M/F ratio (low force) as compared to closed helical loop on 1 mm activation[15]. T-loop can be preferred over closed helical loop, when torque has to be preserved in the anterior segment during retraction in lingual orthodontics.

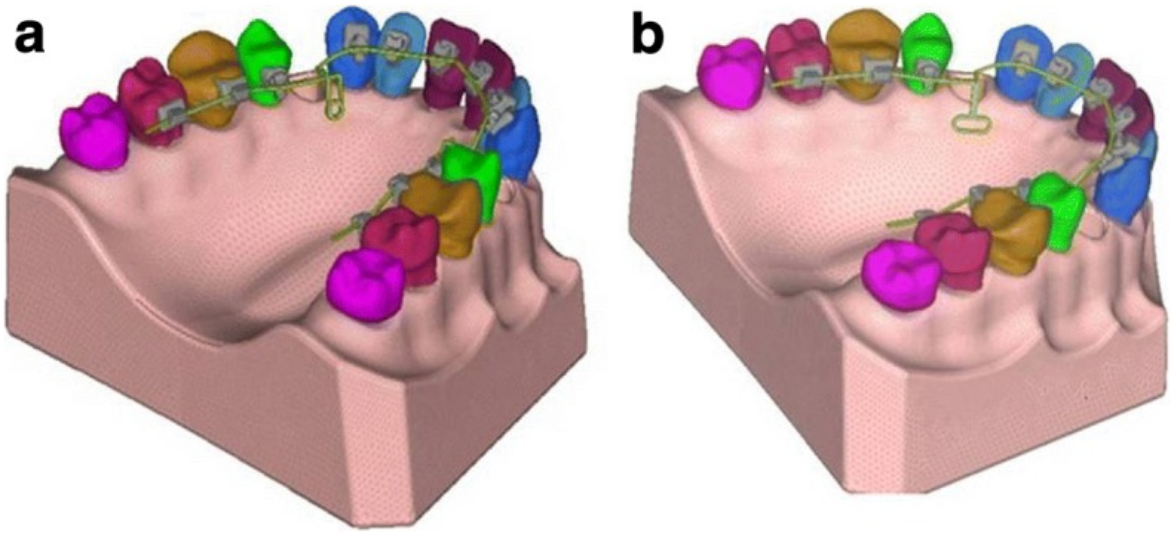

Figure 3: Comparison of closed helical loop and T-loop in lingual orthodontics

Moments & M/F ratios produced by different gabling in the three retraction loops (Tear drop loop, T-loop, Open vertical loop) and movement of the anterior and posterior teeth of the maxillary arch (1 mm activation) were studied[16]. With an increase in angulation of gable bend intrusive, extrusive and horizontal movements increases. All values of T-loop are more than Teardrop loop and less than Open vertical loop. Teardrop loop with 10-20 (α-β) bends is preferable for Group A anchorage.

The effects of elastic modulus, cross-sectional dimensions, loop dimensions, and activation force on the M/F ratio of vertical, L- and T-loops were analysed[17]. M/F ratio of the loop is increased as the loop height increases (more effective in T loop). In vertical loops, increasing the ring radius is more beneficial than increasing the loop height. TMA wire generates a higher M/F ratio due to its lower elastic modulus as compared to SS wire. Small wire cross-sectional area and high force can produce a high M/F ratio.

(4) TEMPORARY ANCHORAGE DEVICE

FEM study was conducted in order to investigate the effect of thread design of a mini-implant on primary stability, strain pattern and magnitude in the surrounding bone structure during orthodontic loading (400 g)[18]. Mini-implants with deeper thread showed more bone strain than mini-implants with less depth. No difference was found between the mini- implant with sharp and blunt edges.

A study was conducted to predict the amount of maxillary molars distalization in nongrowing patients with the skeletal anchorage system (SAS) and the relationship between the amount of distalization and age[19]. The average distalization was 3.78 mm at the crown level and 3.20 mm at the root level. The distalization at the crown level was significantly correlated with the average value of treatment goals (3.60 mm). Molars were predictably distalized without regard to patient age and extraction of the 2nd/3rd molars.

The mechanics of tooth movement patterns for total distalization of the mandibular dentition based on force angulation were studied[20]. Displacement was caused by movement of the whole dentition, elastic deflection of the wire, and clearance gap between the wire and slot. Dentition rotated clockwise or counter clockwise when the force

passed below or above the center of resistance respectively. Elastic deflection of the arch wire tipped anterior teeth lingually.

Stress and displacement effects of maxillary posterior intrusion mechanics with mini-implant were evaluated[21]. Mesio-cervical region (1st molar), the middle third (2nd premolar) and regions of 2nd molar adjacent to force application sites showed high stress levels. Minimum stress was observed in apical region of 1st premolar. Application of 3 mini-implant and trans-palatal arches provide significant true intrusion of maxillary molars with less stress in the apical area.

Stress pattern in the adjacent bone due to root proximity of orthodontic mini-implant with 30° angle and traction force of 2N was examined[22]. Category I: 1mm away from the root, Category II: Part of the screw was embedded in the periodontal membrane, Category III: Part of the screw touched the root. Mini-implant placed away from the root showed least number of stresses. Stress was concentrated near the neck of the mini-implant. Amount of stress is inversely proportional to the distance of mini-implant from root.

OTHER USES:

- To analyse treatment associated morphological changes in facial soft tissue[23].
- As a tool to analyse morphometric craniofacial biology[24].
- To assess the effects of orthodontic forces on the periodontal ligament, alveolar bone and root cementum[25].
- To compare individual tooth movement[26,27,28,29].
- To optimize bracket design[30,31].
- To evaluate bond strength [32,33,34].
- To appreciate basic structures of the materials having complex structures like micro-implants[35,36,37].
- To plan orthognathic surgery[38].

References:

1. Prasad Konda, Tarannum SA, Basic principles of finite element method and its applications in orthodontics JPBMS, 2012, 16 (11).
2. Singh GD, Clark WJ. Localization of mandibular changes in patients with class II division 1 malocclusions treated with twin-block appliances: finite element scaling analysis. American Journal of Orthodontics and Dentofacial Orthopedics. 2001 Apr 1;119(4):419-25.
3. Chaudhry A, Sidhu MS, Chaudhary G, Grover S, Chaudhry N, Kaushik A. Evaluation of stress changes in the mandible with a fixed functional appliance: a finite element study. American Journal of Orthodontics and Dentofacial Orthopedics. 2015 Feb 1;147(2):226-34.

4. Ulusoy Ç, Darendeliler N. Effects of Class II activator and Class II activator high-pull headgear combination on the mandible: a 3-dimensional finite element stress analysis study. American Journal of Orthodontics and Dentofacial Orthopedics. 2008 Apr 1;133(4):490-e9.

5. Tanne K, Lu YC, Tanaka E, Sakuda M. Biomechanical changes of the mandible from orthopaedic chin cup force studied in a three-dimensional finite element model. The European Journal of Orthodontics. 1993 Dec 1;15(6):527-33.

6. Fernandes LC, Vitral RW, Noritomi PY, Schmitberger CA, da Silva Campos MJ. Influence of the hyrax expander screw position on stress distribution in the maxilla: A study with finite elements. American Journal of Orthodontics and Dentofacial Orthopedics. 2019 Jan 1;155(1):80-7.

7. Tanne K, Matsubara S, Sakuda M. Location of the centre of resistance for the nasomaxillary complex studied in a three-dimensional finite element model. British journal of orthodontics. 1995 Aug 1;22(3):227-32.

8. Geramy A. Alveolar bone resorption and the center of resistance modification (3-D analysis by means of the finite element method). American Journal of Orthodontics and Dentofacial Orthopedics. 2000 Apr 1;117(4):399-405.

9. Aruna J. A study on evaluation of center of resistance of maxillary four incisors during simultaneous intrusion and retraction: a finite element study. Journal of pharmacy & bioallied sciences. 2014 Jul;6(Suppl 1):S49.

10. Aruna J. A study on evaluation of center of resistance of maxillary four incisors during simultaneous intrusion and retraction: a finite element study. Journal of pharmacy & bioallied sciences. 2014 Jul;6(Suppl 1):S49.

11. Jo AR, Mo SS, Lee KJ, Sung SJ, Chun YS. Finite-element analysis of the center of resistance of the mandibular dentition. Korean journal of orthodontics. 2017 Jan;47(1):21.

12. Techalertpaisarn P, Versluis A. Mechanical properties of Opus closing loops, L-loops, and T-loops investigated with finite element analysis. American Journal of Orthodontics and Dentofacial Orthopedics. 2013 May 1;143(5):675-83.

13. Safavi MR, Geramy A, Khezri AK. M/F ratios of four different closing loops: 3D analysis using the finite element method (FEM). Australian orthodontic journal. 2006 Nov;22(2):121.

14. Rao PR, Shrivastav SS, Joshi RA. Evaluation and comparison of biomechanical properties of snail loop with that of opus loop and teardrop loop for en masse retraction of anterior teeth: FEM Study. Journal of Indian Orthodontic Society. 2013 Jun;47(2):62-7.

15. Shahroudi AS. The Role of Loop Height and Design on its Force Characteristics in Alignment of Teeth: A Finite Element Analysis. Iranian Journal of Orthodontics. 2016 Jun;11(1).

16. Chacko A, Tikku T, Khanna R, Maurya RP, Srivastava K. Comparative assessment of the efficacy of closed helical loop and T-loop for space closure in lingual orthodontics—a finite element study. Progress in orthodontics. 2018 Dec;19(1):1-8.

17. Kamisetty SK, Raghuveer N, Rajavikram N, Chakrapani N, Dwaragesh P. Evaluation of Effects and Effectiveness of Various α and β Angulations for Three Different Loop Made of Stainless-Steel Arch Wires–A FEM Study. Journal of clinical and diagnostic research: JCDR. 2014 Jul;8(7):ZC33.

18. Cai Y. Finite element analysis of archwire parameters and activation forces on the M/F ratio of vertical, L-and T-loops. BMC oral health. 2020 Dec;20(1):1-2.

19. Sugawara J, Kanzaki R, Takahashi I, Nagasaka H, Nanda R. Distal movement of maxillary molars in nongrowing patients with the skeletal anchorage system. American journal of orthodontics and dentofacial orthopedics. 2006 Jun 1;129(6):723-33.

20. Chae JM, Park JH, Kojima Y, Tai K, Kook YA, Kyung HM. Biomechanical analysis for total distalization of the mandibular dentition: A finite element study. American Journal of Orthodontics and Dentofacial Orthopedics. 2019 Mar 1;155(3):388-97.

21. Pekhale N, Maheshwari A, Kumar M, Kerudi VV, Patil H, Patil B. Evaluation of stress patterns on maxillary posterior segment when intruded with mini-implant anchorage: a three-dimensional finite element study. APOS Trends Orthod. 2016 Jan 1;6:18-23.

22. Handa A, Shetty B, Reddy VP, Hegde N, Koushik HS, Handa JK. Effect of root proximity of orthodontic mini-implant on bone stress: A dimensional finite element analysis. Journal of Indian Orthodontic Society. 2016 Mar;50(1):14-8.

23. Chen S, Xu TM, Lou HD, Rong QG. Individualized three-dimensional finite element model of facial soft tissue and preliminary application in orthodontics. Zhonghua Kou Qiang Yi Xue Za Zhi 2012; 47:730-734

24. Glenn T. Sameshima and Michael Melnick. Finite element based cephalometric analysis. The Angle Orthodontist Oct 1994; 64 (5): 343-50.

25. Viecilli RF, Kar-Kuri MH, Varriale J, Budiman A, Janal M. Effects of initial stresses and time on orthodontic external root resorption. J Dent Res 2013; 92:346-351.

26. Van Schepdael A, Geris L, Vander Sloten J. Analytical determination of stress patterns in the periodontal ligament during orthodontic tooth movement. Med Eng Phys 2013; 35:403-410.

27. Vikram NR, Senthil Kumar KS, Nagachandran KS, Hashir YM. Apical stress distribution on maxillary central incisor during various orthodontic tooth movements by varying cemental and two different periodontal ligament thicknesses: a FEM study. Indian J Dent Res 2012; 23:213-220.

28. Lin YL, Liu YH, Wang DM, Xu JW. Three-dimensional finite element analysis on the effect of posterior cross-bite of individual teeth on temporomandibular joint. Zhonghua Kou Qiang Yi Xue Za Zhi 2013; 48:86-90.

29. Geramy A. Bodily labializing lateral incisors: 3D analysis using finite element method. Acta Odontol Scand 2013; 71:570-576.

30. Huang Y, Keilig L, Rahimi A, Reimann S, Bourauel C. Torque capabilities of self-ligating and conventional brackets under the effect of bracket width and free wire length. Orthod Craniofac Res 2012; 15:255-262.

31. Holberg C, Winterhalder P, Holberg N, Wichelhaus A, Rudzki-Janson I. Orthodontic bracket debonding: risk of enamel fracture.Clin Oral Investig 2014; 18:327-334.

32. Algera TJ, Feilzer AJ, Prahl-Andersen B, Kleverlaan CJ. A comparison of finite element analysis with in vitro bond strength tests of the bracket–cement–enamel system. The European Journal of Orthodontics. 2011 Dec 1;33(6):608-12.

33. Shyagali TR, Bhayya DP, Prakash A, Dungarwal N, Arora A. Comparison of stresses generated by different bracket debonding forces using finite element analysis. Journal of Indian Orthodontic Society. 2012 Jul;46(3):137-40.

34. Elsaka SE, Hammad SM, Ibrahim NF. Evaluation of stresses developed in different bracket-cement-enamel systems using finite element analysis with in vitro bond strength tests. Progress in orthodontics. 2014 Dec;15(1):1-8.

35. K.R. Williams, J.T. Edmundson. Orthodontic tooth movement analysed by the Finite Element Method. Biomaterials 1984; 5(6): 347-351.

36. Jones ML, Hickman J, Middleton J, Knox J, Volp C. A validated finite element method study of orthodontic tooth movement in the human subject. J Orthod 2001; 28: 29–38.

37. Cattaneo PM, Dalstra M, Melsen. The finite element method: a tool to study orthodontic tooth movement. BJ Dent Res. 2005; 84(5): 428-33.

38. Lisiak-Myszke M, Marciniak D, Bieliński M, Sobczak H, Garbacewicz Ł, Drogoszewska B. Application of Finite Element Analysis in Oral and Maxillofacial Surgery—A Literature Review. Materials. 2020 Jan;13(14):3063.

Date of Publication: 25 June 2021
Author Declaration: Source of support: Nil, Conflict of interest: Nil
Was informed consent obtained from the subjects involved in the study? YES
For any images presented appropriate consent has been obtained from the subjects: NA
Plagiarism Checked: Urkund Software

DOI: 10.36848/IJBAMR/2020/29215.55796